Casein kinase 1δ functions at the centrosome and Golgi to promote ciliogenesis

Yoshimi Endo Greer[a], Christopher J. Westlake[b], Bo Gao[c], Kapil Bharti[d], Yoko Shiba[a], Charles P. Xavier[a], Gregory J. Pazour[e], Yingzi Yang[c], and Jeffrey S. Rubin[a]

[a]Laboratory of Cellular and Molecular Biology, National Cancer Institute, Bethesda, MD 20892; [b]Laboratory of Cell and Developmental Signaling, National Cancer Institute, Frederick, MD 21702; [c]Genetic Disease Research Branch, National Human Genome Research Institute, Bethesda, MD 20892; [d]Ophthalmic Genetics and Visual Function Branch, National Eye Institute, Bethesda, MD 20892; [e]Program in Molecular Medicine, University of Massachusetts Medical School, Worcester, MA 01605

ABSTRACT **Inhibition of casein kinase 1 delta (CK1δ) blocks primary ciliogenesis in human telomerase reverse transcriptase immortalized retinal pigmented epithelial and mouse inner medullary collecting duct cells-3. Mouse embryonic fibroblasts (MEFs) and retinal cells from *Csnk1d* (CK1δ)-null mice also exhibit ciliogenesis defects. CK1δ catalytic activity and centrosomal localization signal (CLS) are required to rescue cilia formation in MEFs$^{Csnk1d\ null}$. Furthermore, expression of a truncated derivative containing the CLS displaces full-length CK1δ from the centrosome and decreases ciliary length in control MEFs, suggesting that centrosomal CK1δ has a role in ciliogenesis. CK1δ inhibition also alters pericentrosomal or ciliary distribution of several proteins involved in ciliary transport, including Ras-like in rat brain-11A, Ras-like in rat brain-8A, centrosomal protein of 290 kDa, pericentriolar material protein 1, and polycystin-2, as well as the Golgi distribution of its binding partner, A-kinase anchor protein 450 (AKAP450). As reported for AKAP450, CK1δ was required for microtubule nucleation at the Golgi and maintenance of Golgi integrity. Overexpression of an AKAP450 fragment containing the CK1δ-binding site inhibits Golgi-derived microtubule nucleation, Golgi distribution of intraflagellar transport protein 20 homologue, and ciliogenesis. Our results suggest that CK1δ mediates primary ciliogenesis by multiple mechanisms, one involving its centrosomal function and another dependent on its interaction with AKAP450 at the Golgi, where it is important for maintaining Golgi organization and polarized trafficking of multiple factors that mediate ciliary transport.**

Monitoring Editor
Yixian Zheng
Carnegie Institution

Received: Oct 18, 2013
Revised: Feb 25, 2014
Accepted: Mar 12, 2014

INTRODUCTION

The primary cilium is a conserved, microtubule (MT)-based structure that emanates from the basal body, a membrane-docked mother centriole (Satir and Christensen, 2007; Garcia-Gonzalo and Reiter, 2012). It serves important sensory and signaling functions via membrane proteins specifically localized to its surface. Defects in primary ciliogenesis have been implicated in several genetic disorders, including Bardet–Biedl, Joubert, and Meckel–Gruber syndromes and polycystic kidney disease (Marshall, 2008; Gerdes *et al.*, 2009; Kim and Dynlacht, 2013).

Formation of the primary cilium requires polarized protein transport to the basal body and subsequent incorporation of cargo into the ciliary membrane (Gerdes *et al.*, 2009; Nachury *et al.*, 2010). This process depends on MT networks and various effectors that facilitate vesicle trafficking and subsequent assembly of the ciliary membrane (Berbari *et al.*, 2008; Garcia-Gonzalo *et al.*, 2011). The small GTPase Ras-like in rat brain 11 (Rab11), a mediator of transport in the endocytic recycling compartment and *trans*-Golgi network, has an important role, as it recruits Rabin8 (a Rab8 guanine nucleotide exchange factor) to activate Ras-like in rat brain 8 (Rab8),

This article was published online ahead of print in MBoC in Press (http://www.molbiolcell.org/cgi/doi/10.1091/mbc.E13-10-0598) on March 19, 2014.

The authors declare no competing financial interests.

Address correspondence to: Jeffrey S. Rubin (rubinj@mail.nih.gov).

Abbreviations used: AKAP450, A-kinase anchor protein 450; CEP290, centrosomal protein of 290 kDa; CK1, casein kinase 1; CLS, centrosomal localization signal; GFP, green fluorescent protein; hTERT-RPE, human telomerase reverse transcriptase immortalized retinal pigmented epithelial; IFT20, intraflagellar transport protein 20 homologue; MEF, mouse embryonic fibroblast; mIMCD3, mouse inner medullary collecting duct cells-3; MT, microtubule; PCM1, pericentriolar material protein 1; Rab8, Ras-like in rat brain-8; Rab11, Ras-like in rat brain-11; WT, wild type.

which promotes the fusion of vesicles containing cilia-bound cargo into the nascent ciliary membrane (Knodler *et al.*, 2010; Westlake *et al.*, 2011; Hsiao *et al.*, 2012). The axonemal cytoskeleton of the cilium is assembled via a process called intraflagellar transport that is mediated by large protein complexes known as intraflagellar transport protein particles (Pedersen and Rosenbaum, 2008). Intraflagellar transport protein 20 homologue (IFT20) is a component of IFT particles that also is present in the Golgi complex, where it facilitates the transport of ciliary membrane proteins such as polycystin-2 to the pericentrosomal region (Follit *et al.*, 2006).

Several ciliopathy proteins—factors required for cilia formation or function—are located at centriolar satellites (Lopes *et al.*, 2011). For instance, centrosomal protein of 290 kDa (CEP290)/NPHP6 functions in ciliary transport and organization of the MT network (Kim *et al.*, 2008; Coppieters *et al.*, 2010). Pericentriolar material protein 1 (PCM1), a CEP290-binding protein, assists in anchoring MTs and recruiting several key centrosomal components (e.g., centrin, pericentrin, and ninein) and various ciliopathy proteins, such as BBS4 and OFD1, to the centrosomal or pericentrosomal area (Dammermann and Merdes, 2002; Lopes *et al.*, 2011; Stowe *et al.*, 2012).

Casein kinase 1δ (CK1δ) is an evolutionarily conserved serine/threonine kinase that participates in diverse cellular processes, including vesicle trafficking, DNA repair, chromosome segregation, cell cycle progression, circadian rhythm, Wnt signaling, and neurite outgrowth (Gross and Anderson, 1998; Knippschild *et al.*, 2005; Bischof *et al.*, 2011; Cheong and Virshup, 2011; Greer and Rubin, 2011). CK1δ localizes to the centrosome, *trans*-Golgi network (TGN), and cytoplasmic vesicles (Behrend *et al.*, 2000; Greer and Rubin, 2011; Jakobsen *et al.*, 2011). Its centrosomal location is required for Wnt3a-dependent neuritogenesis in TC-32 Ewing sarcoma cells (Greer and Rubin, 2011). Recently a CK1δ binding partner, A-kinase anchor protein 450 (AKAP450)/centrosomal Golgi N-kinase anchoring protein, was implicated in ciliogenesis through its regulation of Golgi positioning, integrity, and the nucleation of MTs at the Golgi (Rivero *et al.*, 2009; Hurtado *et al.*, 2011).

Here we report that CK1δ is a mediator of ciliogenesis in several model systems. Its role in ciliogenesis involves functions at both the centrosome and the Golgi, the latter associated with AKAP450, Golgi-derived MT nucleation, Golgi organization, and directed protein trafficking. Inhibition of CK1δ expression or kinase activity disrupted the intracellular distribution of many effectors of ciliogenesis, including Rab11a, Rab8a, CEP290, PCM1, AKAP450, and IFT20. Its effect on ciliogenesis likely depends on a multifaceted regulation of MT networks and vesicle trafficking required for ciliary transport.

RESULTS

CK1δ mediates ciliogenesis in multiple model systems

We initially determined whether CK1δ participates in ciliogenesis by treating human telomerase reverse transcriptase immortalized retinal pigmented epithelial (hTERT-RPE) cells with small interfering RNA (siRNA). After 48 h of serum starvation, 85.0% of cells incubated with negative control luciferase (Luc) siRNA displayed a primary cilium. Only 38.8% of cells exposed to CK1δ siRNA were ciliated, whereas the percentage of ciliated cells was not affected by siRNA directed against the highly related enzyme CK1ε (Figure 1, A and B). Western blot analysis confirmed the specificity of siRNA knockdown reagents (Figure 1C). Similar results were obtained with multiple different siRNA reagents targeting CK1δ and CK1ε (unpublished data). The contrast in activity of CK1 isoforms was consistent with the preferential localization of CK1δ at the centrosome (Supplemental Figure S1, A and B). Using a CK1δ/ε kinase inhibitor, PF670462, we observed a dose-dependent reduction in the percentage of ciliated hTERT-RPE cells (Figure 1D). At lower concentrations (0.3 and 1.0 μM), primary cilia were still present in >60% of cells; however, ciliary length was shortened (Figure 1E). PF670462 also decreased ciliary length in mouse inner medullary collecting duct cells-3 (mIMCD3; Supplemental Figure S1, C and D), another line commonly used in studies of ciliogenesis.

To ensure that observations made with the siRNA reagents and kinase inhibitor were due to on-target effects, we performed experiments with mouse embryo fibroblasts (MEFs) homozygous for a CK1δ floxed allele (Etchegaray *et al.*, 2009). Whereas 77.1% of MEF cells infected with negative control adenovirus expressing GFP contained a primary cilium, only 29.1% of MEF cells treated with adenovirus expressing Cre and lacking CK1δ were ciliated (Figure 2, A–C). Moreover, examination of retinal tissue from late-gestational wild-type (WT) versus *Csnk1d*-null embryos revealed a decline in ciliary length of neural progenitor and RPE cells when CK1δ was absent (Supplemental Figure S2). Taken together, these results demonstrated that CK1δ has a significant role in ciliogenesis.

Structure–function analysis of CK1δ in MEF primary ciliogenesis

CK1δ contains a kinase domain comprising approximately two-thirds of its sequence and a centrosomal localization signal (CLS) located in its C-terminal domain. To investigate the function of these domains in ciliogenesis, we generated various CK1δ constructs, including ones encoding Myc-tagged, full-length WT CK1δ, full-length CK1δ with a K38A substitution that lacks kinase activity (DeMaggio *et al.*, 1992; Fish *et al.*, 1995; Murakami *et al.*, 1999), a truncated derivative missing the C-terminal domain (ΔC), and a derivative containing only the C-terminal domain fused to enhanced GFP (δCT-EGFP; Figure 2, D and E; Greer and Rubin, 2011). Consistent with the data summarized in Figure 2B, cilia were absent or shorter in $MEF^{Csnk1d\ null}$ cells transiently transfected with pcDNA3.3 empty vector compared with $MEF^{Ctl.}$ cells (Figure 2F). Transient transfection of CK1δ WT restored cilia to 80% of cells (44/55) and ciliary length to a level matching that of $MEF^{Ctl.}$ cells. In contrast, none of the other derivatives was able to rescue the ciliary defect (Figure 2F). This confirmed that the catalytic activity of CK1δ was required for optimal cilia formation, as implied by the experiments with PF670462. It also indicated that kinase activity was not sufficient for normal cilia formation, as the C-terminal domain containing the CLS also was necessary to restore ciliogenesis.

To investigate a potential requirement for centrosomal CK1δ in ciliogenesis, we transiently transfected $MEF^{Ctl.}$ cells with δCT-EGFP, which previously was shown to displace full-length CK1δ from the centrosome of TC-32 cells (Greer and Rubin, 2011). Expression of δCT-EGFP significantly reduced ciliary length, whereas εCT-EGFP did not (Figure 2, G and H). Consistent with our earlier results with TC-32 cells, when $MEF^{Ctl.}$ cells were cotransfected with full-length Myc-CK1δ WT and either δCT-EGFP or EGFP, Myc-CK1δ was displaced from the centrosome only in the presence of δCT-EGFP and not displaced from other subcellular compartments such as the Golgi (Supplemental Figure S3). These observations suggested that the centrosomal localization of CK1δ was critical for ciliogenesis.

CK1δ regulates Rab11a/Rab8a distribution

We tested the hypothesis that disruption of CK1δ expression affected the distribution and function of Rab11a and Rab8a in primary ciliogenesis. GFP-Rab11a stably expressed in hTERT-RPE cells was detected at the base of primary cilia (Figure 3, A and B), consistent

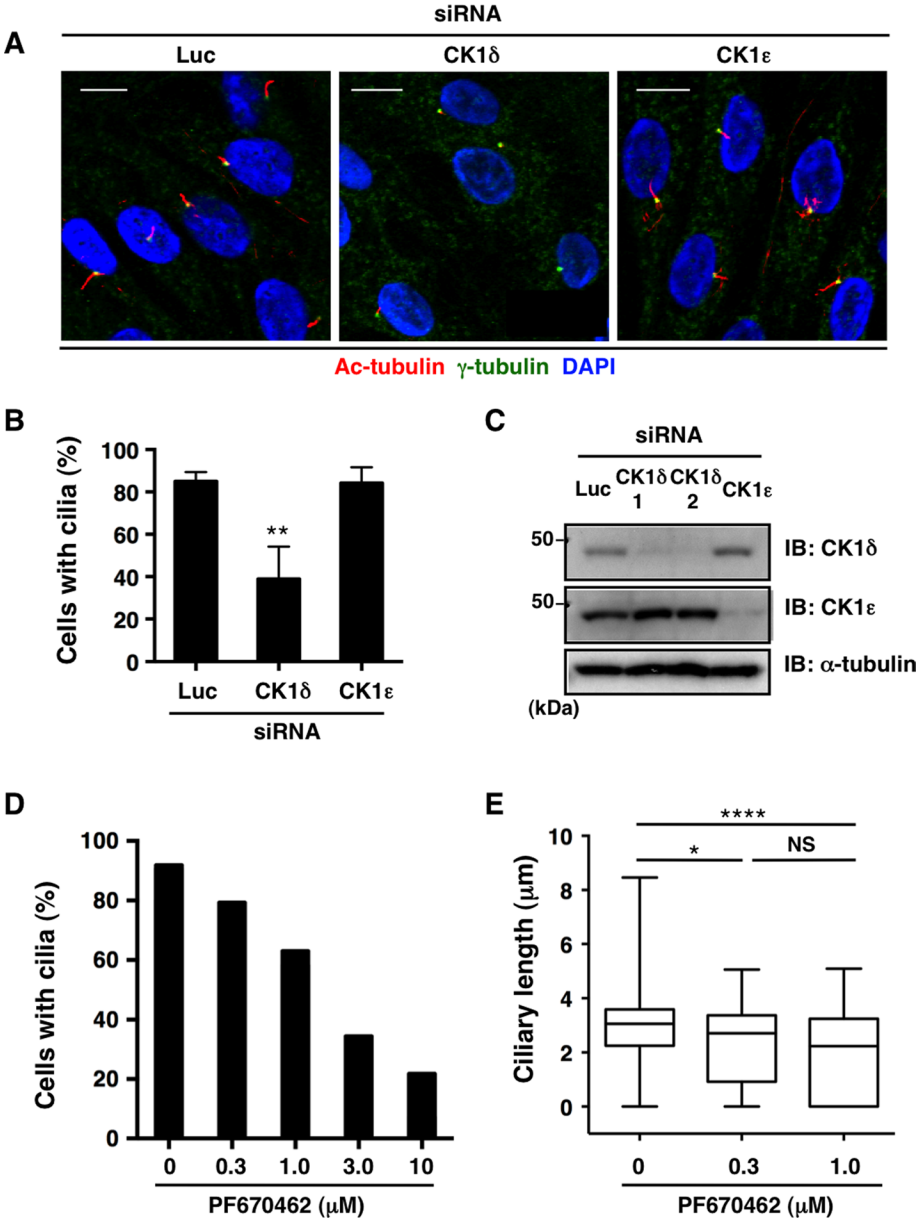

FIGURE 1: CK1δ mediates primary ciliogenesis in hTERT-RPE cells. (A) Representative confocal micrographs of hTERT-RPE cells treated with siRNA reagents targeting luciferase (negative control), CK1δ, or CK1ε. Acetylated tubulin antibody (red) highlights the cilium, γ-tubulin (green) is a centrosomal marker, and DAPI (blue) stains the nucleus. Overlap of acetylated tubulin and γ-tubulin signal is yellow. Bars, 10 μm. (B) Quantitative analysis of data in A. Bar graph and error bars represent mean ± SD from three independent experiments. $^{**}p = 0.007$ (*t* test, compared with Luc siRNA). (C) Western blot analysis of CK1δ and CK1ε in hTERT-RPE whole-cell lysates 72 h after transfection with indicated siRNA reagents. Immunoblot of α-tubulin served as a loading control. (D) Dose-dependent effect of CK1δ/ε kinase inhibitor PF670462 on percentage of cells with primary cilium. Sample number $N = 316$, 117, 247, 78, and 217 cells examined in 0, 0.3, 1.0, 3.0, and 10 μM treatment groups, respectively. (E) Dose-dependent effect of PF670462 on ciliary length. Box represents middle 50% of values for ciliary length; line inside the box indicates median value; and whiskers show upper 25% and lower 25% of values. $N = 99$, 117, and 98 cells examined in 0, 0.3, and 1.0 μM treatment groups, respectively. One-way ANOVA, $p < 0.0001$; Tukey's test, $^{*}p = 0.0177$, $^{****}p < 0.0001$, NS = not significant. See also Supplemental Figure S1.

with previous reports (Westlake *et al.*, 2007; Knodler *et al.*, 2010). CK1δ siRNA markedly disrupted this pattern, as the GFP signal often was diffuse or undetectable. The diminished GFP staining may result from dispersion of GFP-Rab11a due to impaired membrane association rather than increased degradation, as Western blot analysis indicated that the protein level in whole-cell lysates was unchanged (unpublished data). CK1ε siRNA did not affect the pericentrosomal localization of GFP-Rab11a (unpublished data). Furthermore, the ciliary distribution of GFP-Rab8a also was inhibited by knockdown of CK1δ but not CK1ε (Figure 3, C and D).

CEP290 and PCM1 distribution in centriolar satellites is inhibited by CK1δ siRNA

Because CEP290 interacts with PCM1 and is required for Rab8 localization to the primary cilium (Kim *et al.*, 2008), we investigated the effect of CK1δ siRNA on their distribution in hTERT-RPE cells. CEP290 punctae coincided with the centrosomal marker pericentrin and were scattered beyond it in control cells treated with Luc siRNA (Figure 4A). CK1δ knockdown resulted in substantial decrease in the number of punctae near the centrosome, although there still was overlap of CEP290 and pericentrin staining (Figure 4, A and B). CK1ε knockdown did not alter the basic staining pattern of CEP290 (Figure 4, A and B). PCM1 also had a pericentrosomal distribution, which was strikingly dispersed by CK1δ but not CK1ε siRNA (Figure 4, C and D). CEP290 and PCM1 protein levels in whole-cell lysates were similar in the various siRNA treatment groups (Figure 4E), suggesting that the diminished signal intensities associated with CK1δ siRNA were due to intracellular dispersion of the proteins rather than degradation. The pericentrosomal localization of CEP290 and PCM1 also was perturbed in MEF$^{Csnk1d\ null}$ cells (Supplemental Figure S4). However, PCM1 localization was not disrupted by δCT-EGFP (Supplemental Figure S5A), implying that centrosomal CK1δ was not important for PCM1 subcellular targeting. Thus our results indicate that CK1δ is required for proper positioning of these centriolar satellite proteins, although the mechanism does not involve centrosomal CK1δ.

AKAP450 distribution is dispersed by CK1δ inhibition

We also examined the effect of CK1δ on the intracellular distribution of its binding partner AKAP450 because AKAP450 has a role in ciliogenesis (Hurtado *et al.*, 2011). AKAP450 colocalized with the centrosomal marker γ-tubulin and the *cis*-Golgi marker GM130 in hTERT-RPE cells (Figure 5A). The AKAP450 signal was dramatically reduced in cells transfected with CK1δ siRNA (Figure 5B). PF670462 also decreased AKAP450 signal intensity, particularly at the Golgi (Figure 5C). As with CEP290 and PCM1, Western blot analysis indicated that CK1δ

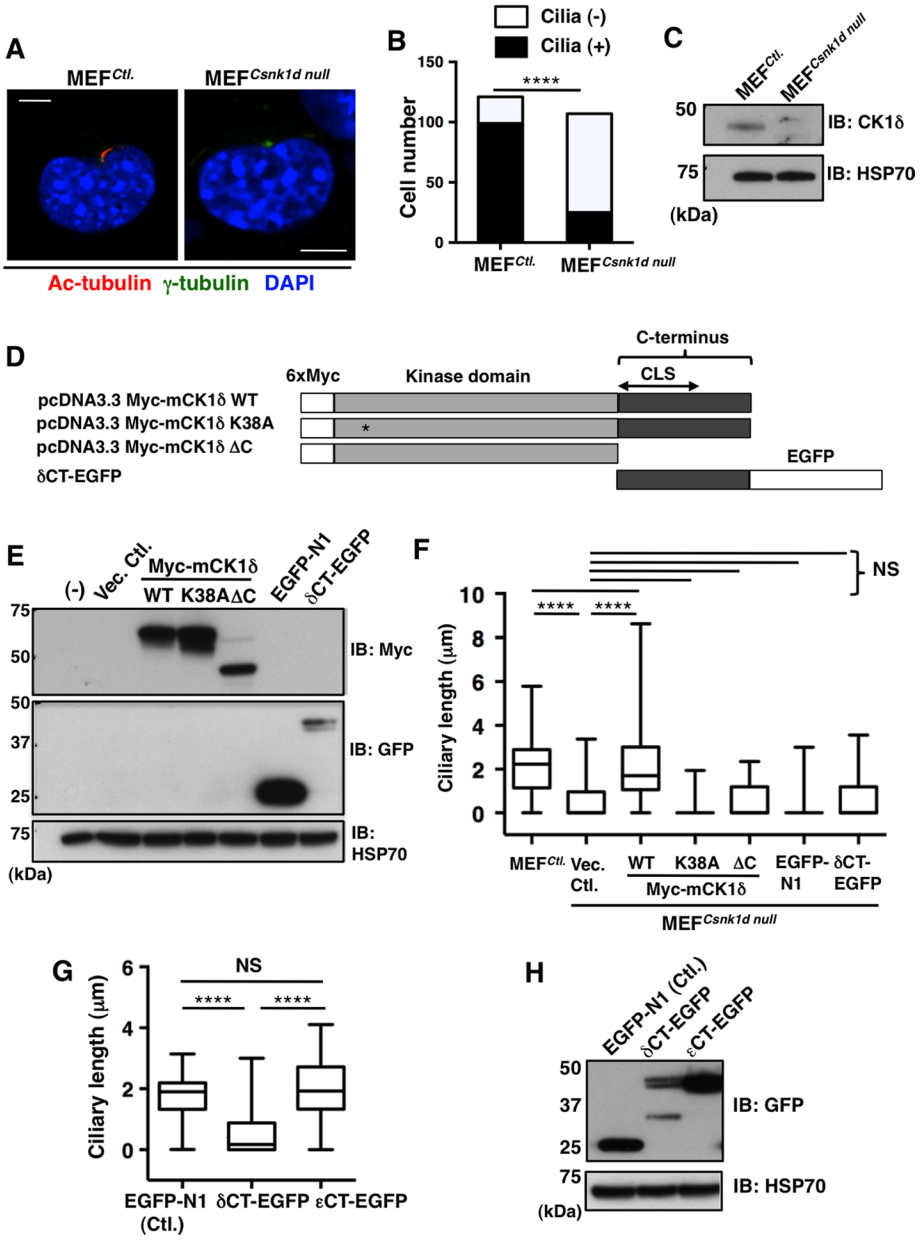

FIGURE 2: Structure–function analysis of CK1δ using MEF model of primary ciliogenesis. (A) Representative confocal micrographs of cells stained to detect cilia. MEF cells homozygous for the floxed *Csnk1d* allele and infected with adenovirus expressing GFP (MEF$^{Ctl.}$) or Cre recombinase (MEF$^{Csnk1d\ null}$) were processed to visualize the primary cilium. Markers are as described in the legend to Figure 1A. Bars, 5 μm. (B) Quantitative analysis of data in A. Number of cells with or without primary cilium is indicated. ****$p < 0.0001$ (Fisher's exact test). (C) Western blot analysis of CK1δ in MEFs homozygous for floxed *Csnk1d* allele and infected with adenovirus expressing GFP (Ctl.) or Cre recombinase. (D) Schematic diagram of CK1δ derivatives. Myc-tagged wild-type mouse CK1δ, kinase-inactive point mutant (K38A, marked with asterisk), C-terminal truncation mutant (ΔC), and EGFP fusion protein containing the C-terminal domain with centrosomal localization signal (CLS). (E) Western blot analysis of CK1δ derivatives and EGFP-N1 expressed in MEF$^{Csnk1d\ null}$ cells. (F) Ciliary length in MEF$^{Csnk1d\ null}$ cells transfected with various CK1δ derivatives or EGFP-N1 control construct. $N = 106$, 93, 55, 46, 47, 50, and 51 cells for treatment groups from left to right. One-way ANOVA, $p < 0.0001$; Tukey's test, ****$p < 0.0001$, NS = not significant. (G) Ciliary length in MEF$^{Ctl.}$ cells transfected with EGFP-N1 or the EGFP fusion proteins containing the C-terminal domain of CK1δ vs. CK1ε. $N = 30$, 30, and 41 cells for Ctl., δCT-EGFP, and εCT-EGFP transfectants, respectively. One-way ANOVA, $p < 0.0001$; Tukey's test, ****$p < 0.0001$, NS = not significant. (H) Western blot analysis of MEF$^{Ctl.}$ cells transfected with EGFP fusion constructs. See also Supplemental Figure S2.

siRNA did not alter the AKAP450 protein content in whole-cell lysates (Figure 4E), implying that the decline in signal intensity was due to dispersion of AKAP450 in the cell. A similar decrease in signal intensity at the centrosome and Golgi was observed in MEF$^{Csnk1d\ null}$ cells (Figure 5D). These results demonstrate that the normal intracellular distribution of AKAP450 depends on the expression and catalytic activity of CK1δ.

CK1δ inhibition disrupts *cis*-Golgi organization, IFT20 distribution, and Golgi-derived MT nucleation

Because AKAP450 functions at the *cis*-Golgi to maintain the ribbon structure and location of the Golgi near the centrosome, we investigated the possibility that CK1δ inhibition would alter the architecture and position of the Golgi apparatus. In hTERT-RPE cells transfected with Luc siRNA, GM130 was observed in a highly polarized, ribbon structure around the centrosome (Figure 5E), a pattern that is critical for directional protein transport (Yadav *et al.*, 2009). Strikingly, the polarized ribbon structure of GM130 was lost in hTERT-RPE cells transfected with CK1δ siRNA (Figure 5E). To further characterize this phenotype, we measured the Golgi diameter and distance between the centrosome and the center of a circle circumscribing the Golgi (Hurtado *et al.*, 2011). CK1δ siRNA significantly increased the Golgi diameter and centrosome–Golgi distance (Figure 5, F and G). Similar changes in Golgi positioning and morphology were observed when hTERT-RPE cells were treated with PF670462 and in MEF$^{Csnk1d\ null}$ cells (Figure 5, H and I). Supporting the idea that these changes were independent of centrosomal CK1δ, expression of δCT-EGFP in MEF$^{Ctl.}$ cells did not alter the GM130 staining pattern (Supplemental Figure S5B).

IFT20 is primarily associated with the *cis* and medial cisternae of the Golgi complex, where it functions in the delivery of ciliary membrane proteins from the Golgi complex to the cilium (Follit *et al.*, 2006). Knockdown of CK1δ in hTERT-RPE cells stably expressing GFP-tagged IFT20 disrupted the intracellular distribution of IFT20 (Figure 6A), consistent with perturbation of the GM130 staining pattern (Figure 6A). Similar results were obtained when mIMCD3 cells expressing IFT20-GFP were treated with PF670462 (Figure 6B). In addition, the kinase inhibitor decreased the accumulation of polycystin-2 at the centrosome of

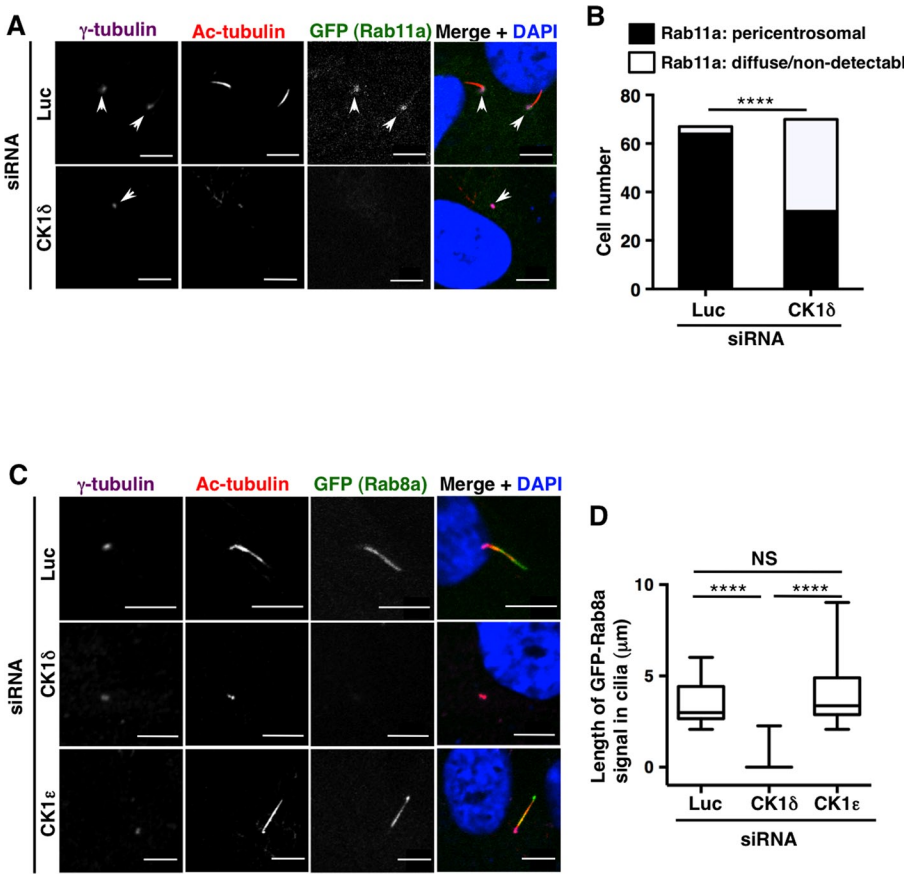

FIGURE 3: CK1δ siRNA disrupts pericentrosomal distribution of GFP-Rab11a and ciliary localization of GFP-Rab8a. (A) Localization of GFP-Rab11a, γ-tubulin, and acetylated tubulin in hTERT-RPE cells stably expressing GFP-Rab11a. After transfection with siRNA reagents, cells were serum starved for 48 h and stained as noted. Arrows indicate centrosomal location. Bars, 5 μm. (B) Quantitative analysis of results in A. ****$p < 0.0001$ (Fisher's exact test). (C) Localization of GFP-Rab8a, γ-tubulin, and acetylated tubulin in hTERT-RPE cells stably expressing GFP-Rab8a. After transfection with siRNA reagents, cells were serum starved for 48 h and stained as indicated. Bars, 5 μm. (D) Quantitative analysis of results in C. $N = 35$, 26, and 23 cells for Luc, CK1δ, and CK1ε siRNA transfectants, respectively. One-way ANOVA, $p < 0.0001$; Tukey's test, ****$p < 0.0001$. Bars, 5 μm.

mIMCD3 cells (Figure 6, C and D), suggesting a defect in IFT20-dependent transport from the Golgi.

The ribbon structure and positioning of the Golgi are highly dependent on MTs (Thyberg and Moskalewski, 1999). Whereas the centrosome is the major site for MT nucleation, Golgi-derived MTs are required for normal Golgi morphology and polarized vesicle transport (Efimov *et al.*, 2007). Golgi MT nucleation is mediated by AKAP450 (Rivero *et al.*, 2009). Therefore we explored the idea that dispersion of AKAP450 and disruption of Golgi structure and positioning were associated with a defect in MT nucleation at the Golgi. Nocodazole treatment followed by washout enabled us to visualize MT asters arising from Golgi fragments stained with GM130 antibody (Figure 7). In contrast to the hTERT-RPE cells transfected with Luc or CK1ε siRNA, knockdown of CK1δ expression inhibited MT formation at the Golgi (Figure 7). Centrosomal MT nucleation appeared to be only partially inhibited in CK1δ-depleted cells. Similar results were obtained with hTERT-RPE cells pretreated with PF670462 (Supplemental Figure S6). Our results indicate that CK1δ is required for normal AKAP450 and IFT20 localization and MT nucleation at the Golgi.

CK1δ-binding AKAP450 fragment disrupts IFT20 Golgi distribution, Golgi MT nucleation, and ciliogenesis

To test the functional relevance of CK1δ/AKAP450 interaction, we generated a GFP-tagged AKAP450 fragment containing the CK1δ-binding site (AKAP450/3315-3496; Sillibourne *et al.*, 2002). For comparison, we also prepared GFP-tagged AKAP450 derivatives containing the GM130-binding site (AKAP450/159-463; Hurtado *et al.*, 2011) or the PACT domain (AKAP450/3643-3908; Gillingham and Munro, 2000), the latter accounting for AKAP450 binding to the centrosome (Figure 8, A and B). As expected, expression of AKAP450/159-463 in MEF$^{Ctl.}$ cells disrupted the Golgi distribution pattern of endogenous AKAP450 while leaving the centrosomal localization intact (Supplemental Figure S7A). Expression of the PACT domain perturbed the centrosomal distribution of endogenous AKAP450, but the Golgi pattern was unaffected (Supplemental Figure S7A). The AKAP450 fragment containing the CK1δ-binding domain altered the distribution of endogenous AKAP450 at both sites, resulting in a diffuse pattern of cytoplasmic staining (Supplemental Figure S7A). Expression of this fragment also resulted in a more diffuse staining pattern for endogenous CK1δ (Supplemental Figure S7B). AKAP450/3315-3496 expression in MEF^{Ctl} cells altered the GM130 staining pattern and decreased the association of IFT20 with GM130 (Figure 8, C and D). Similar results were obtained with mIMCD3 cells (unpublished data).

Next we examined the effect of the AKAP450 fragments on Golgi-derived MT nucleation and ciliogenesis in MEF$^{Ctl.}$ cells (Figure 8, E and F). Expression of AKAP450/159-463 blocked Golgi MT growth after nocodazole washout and decreased ciliary length. These results were consistent with previous work (Hurtado *et al.*, 2011), reinforcing the view that AKAP450-GM130 interaction enables MT nucleation at the Golgi and consequently ciliogenesis. AKAP450/3643-3908 blocked neither MT nucleation nor ciliogenesis, implying that centrosomal AKAP450 is not required for Golgi-derived MT regrowth or ciliogenesis. Finally, AKAP450/3315-3496 inhibited MT nucleation at the Golgi and sharply reduced ciliary length. These data suggest that direct interaction between CK1δ and AKAP450 is necessary for MT nucleation at the Golgi and ciliogenesis.

DISCUSSION

In the present study we demonstrated that CK1δ contributes to ciliogenesis in several models, including cell lines, primary MEF cells, and embryonic tissue from mouse. We originally hypothesized that centrosomal CK1δ would have a role in ciliogenesis because its centrosomal location is critical for Wnt3a-dependent neurite outgrowth in TC-32 cells (Greer and Rubin, 2011). Our present findings are consistent with this idea, as a CK1δ construct lacking the CLS was unable to rescue ciliogenesis in MEF$^{Csnk1d\ null}$ cells, and another

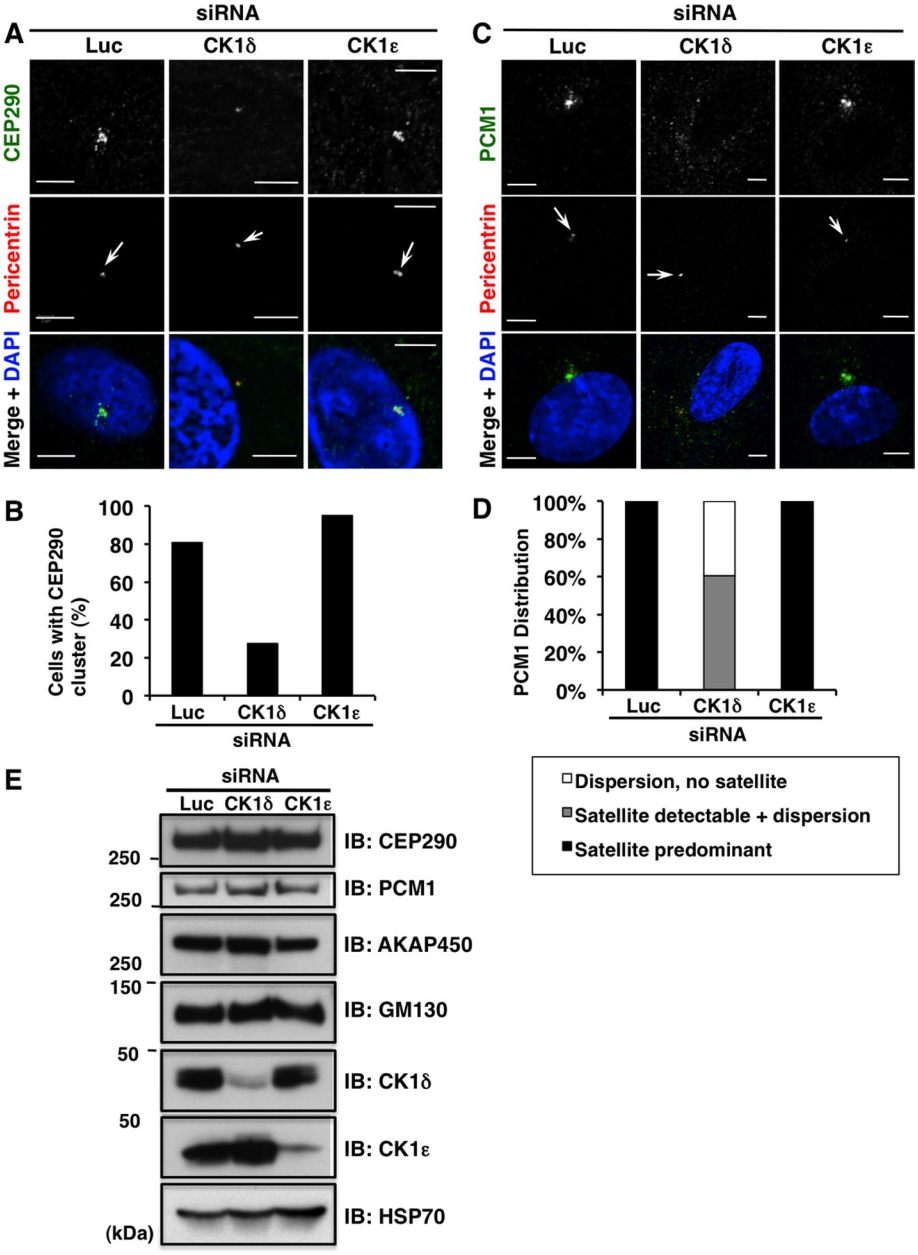

FIGURE 4: CK1δ siRNA disrupts pericentrosomal distribution of CEP290 and PCM1 in hTERT-RPE cells. (A) Intracellular distribution of CEP290. One day after transfection with the indicated siRNA reagents, cells were serum starved for 48 h before staining. Pericentrin served as a centrosomal marker. Bars, 5 μm. (B) Quantitative analysis of data in A. CEP290 cluster was defined by the presence of at least three punctae. $N = 21$, 47, and 20 cells for Luc, CK1δ, and CK1ε siRNA treatment groups, respectively. (C) Intracellular distribution of PCM1. Cells were processed as described in A. Bars, 5 μm. (D) Quantitative analysis of data in C. The distribution pattern was analyzed by classifying cells into three categories: pericentrosomal satellite distribution was strong (black); pericentrosomal distribution was detectable, but cytoplasmic distribution also was present (gray); cytoplasmic distribution without any pericentrosomal staining (white). $N = 14$, 33, and 12 cells for Luc, CK1δ, and CK1ε siRNA treatment groups, respectively. (E). Western blot analysis of endogenous CEP290, PCM1, AKAP450, and GM130 expression in hTERT-RPE cells transfected with CK1δ, CK1ε, or Luc siRNA. Cells were harvested 72 h after siRNA transfection, and equivalent amounts of cell lysates were probed with the indicated antibodies. Isoform-specific knockdown of the CK1 enzymes was confirmed. HSP70 was a loading control.

construct containing the CLS displaced CK1δ from the centrosome of MEF$^{Ctl.}$ cells and inhibited cilia formation (Figure 2 and Supplemental Figure S3). In addition, we found that ciliogenesis depends on CK1δ interaction with AKAP450, which is associated with Golgi-derived MT nucleation and Golgi organization. Disruption of CK1δ expression results in a pattern of protein mislocalization that likely is due to defective trafficking from the Golgi and perhaps elsewhere. We believe that CK1δ functions to coordinate the positioning and activity of multiple ciliary effectors, such as Rab11a and Rab8a, CEP290, PCM1, and IFT20, to mediate transport of polycystin-2 and other membrane cargo from the Golgi to the basal body and nascent cilium (Supplemental Figure S8).

Previous work demonstrated that CK1δ binds to AKAP450 (Sillibourne *et al.*, 2002), but the present study provides the first evidence that their interaction is functionally important. Suppression of CK1δ expression in hTERT-RPE and MEF cells mimicked the effects of AKAP450 knockdown on Golgi organization and Golgi-derived MT nucleation (Rivero *et al.*, 2009), suggesting that CK1δ and AKAP450 are key components of a common mechanism. Knockdown of CK1δ and inhibition of its kinase activity each resulted in dispersion of AKAP450 from its usual polarized perinuclear distribution. This is most likely caused by defects in Golgi positioning, as demonstrated by scattering of the *cis*-Golgi marker GM130. Additional experiments indicated that association of AKAP450 and GM130 was not affected by CK1δ siRNA (unpublished data). CK1δ siRNA also caused loss of AKAP450 from the centrosome, an effect that was not evident after treatment with the kinase inhibitor PF670462. Although detailed understanding of CK1δ activity in regulating MT nucleation and related Golgi organization requires further investigation, the ability of an AKAP450 fragment containing the CK1δ-binding site to disrupt Golgi-derived MT nucleation, GM130 and IFT20 distribution, and ciliogenesis indicates that the interaction between CK1δ and AKAP450 is important for these processes.

Typically, we only observed partial inhibition of ciliogenesis after blockade of CK1δ expression or kinase activity. This might be due to incomplete suppression of CK1δ expression or catalytic activity or to the presence of redundant mechanisms. CK1α1 has been detected in centrosomal preparations but not linked to cilia formation (Jakobsen *et al.*, 2011). CK1γ was identified as a mediator of Rab11-dependent polarized vesicle trafficking in *Drosophila*, although there was no indication that it has a role in ciliogenesis (Gault *et al.*, 2012). CK1ε activates minus end–directed transport of pigment granules along MTs in *Xenopus* melanophores (Ikeda *et al.*, 2011). However, despite this function in transport, our results

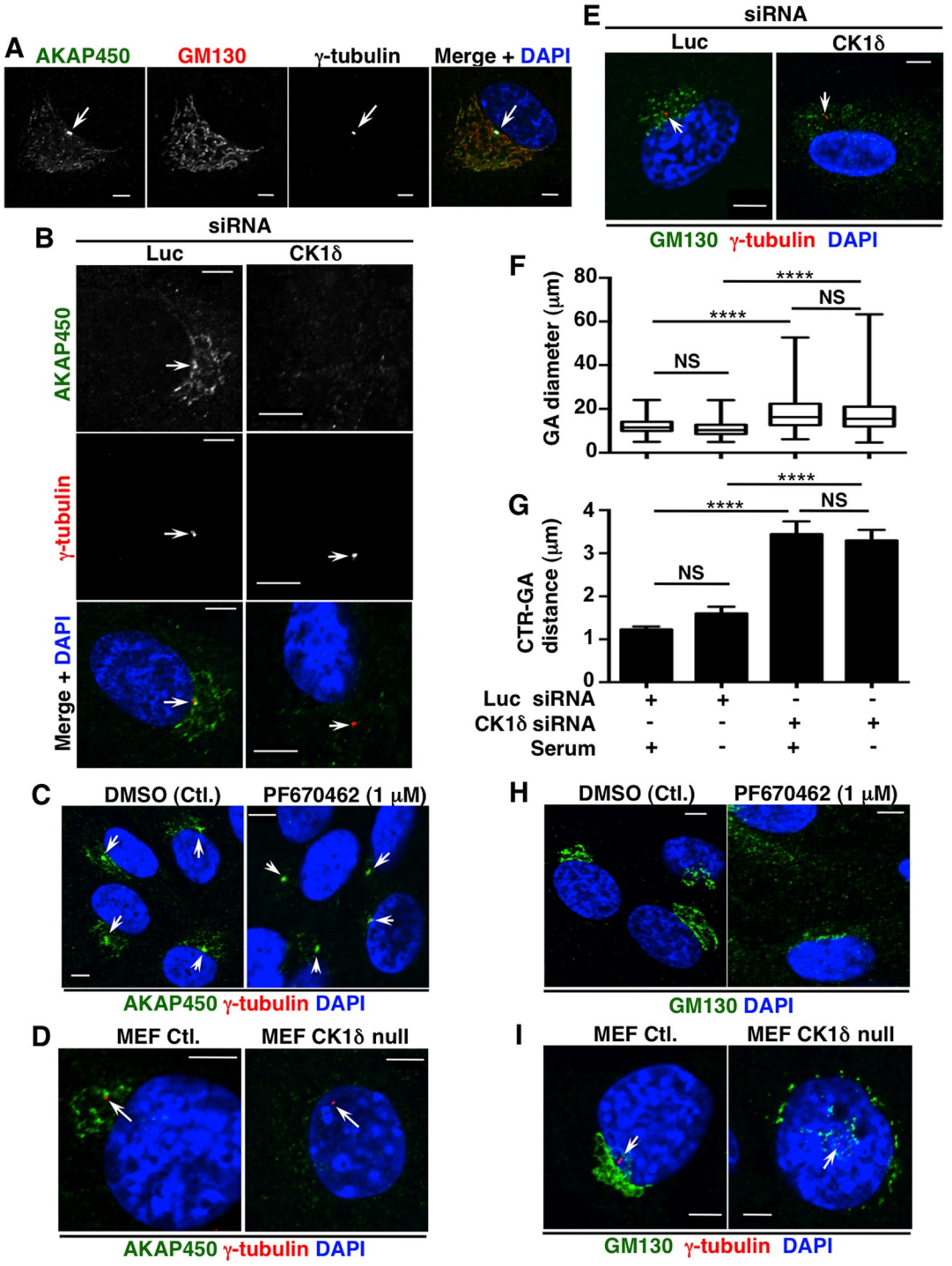

FIGURE 5: Intracellular distribution of AKAP450 and GM130 is regulated by CK1δ. (A) AKAP450 distribution in hTERT-RPE cells cultured with normal growth medium. GM130 and γ-tubulin were markers for *cis*-Golgi and centrosome, respectively. Arrows indicate the centrosome; bars, 5 μm (A–D). (B) AKAP450 distribution in hTERT-RPE cells treated with luciferase or CK1δ siRNA. Cells were maintained in serum-free medium and fixed 72 h after siRNA transfection. (C) AKAP450 distribution in hTERT-RPE cells treated with PF670462 or DMSO. Cells were maintained in serum-free medium with the indicated reagents for 48 h. (D) AKAP450 distribution in $MEF^{Ctl.}$ and $MEF^{Csnk1d\ null}$ cells cultured in growth medium and stained as indicated. (E) GM130 localization in hTERT-RPE cells treated with luciferase or CK1δ siRNA. Cells were maintained in serum-free medium and fixed 72 h after siRNA transfection. Arrows indicate the centrosome; bars, 5 μm (E, H, I). (F) Golgi diameter in cells transfected with CK1δ or luciferase siRNA in presence or absence of serum. $N = 123$, 110, 111, and 155 cells in treatment groups from left to right. One-way ANOVA, $p < 0.0001$; Tukey's test, ****$p < 0.0001$, NS = not significant. (G) Centrosome–Golgi distance in cells treated as described in F. N as in F. Data are presented as mean ±SEM. One-way ANOVA: $p < 0.0001$; Tukey's test, ****$p < 0.0001$, NS = not significant. (H) GM130 distribution in hTERT-RPE cells after PF670462 or dimethyl sulfoxide treatment. Cells were maintained in serum-free medium with the indicated reagents for 48 h. (I) GM130 distribution in $MEF^{Ctl.}$ and $MEF^{Csnk1d\ null}$ cells in growth medium and stained as indicated.

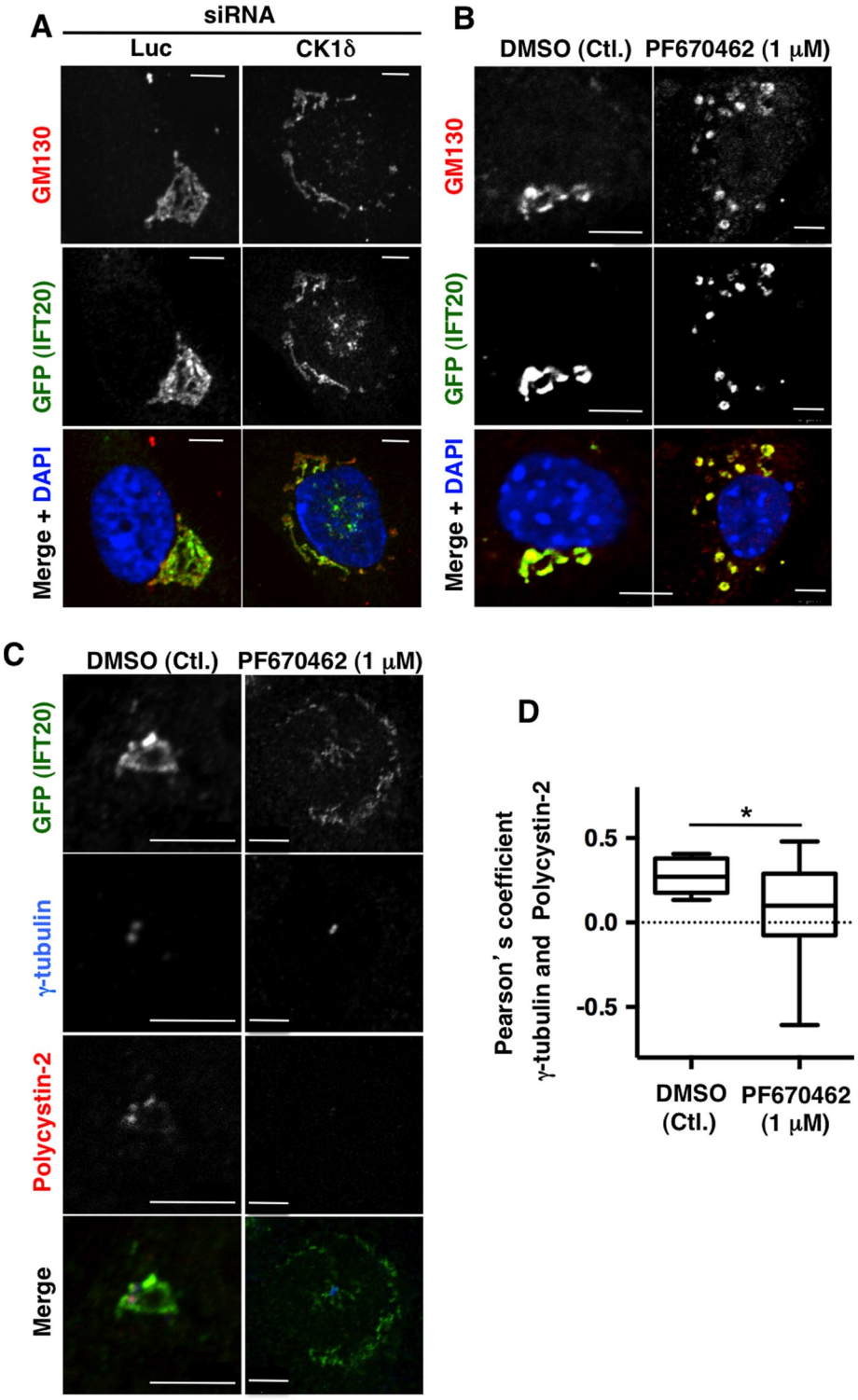

FIGURE 6: IFT20 and polycystin-2 localization are disrupted by CK1δ siRNA and PF670462. (A) GM130 and IFT20 localization in RPE cells expressing IFT20-GFP. Cells were maintained in serum-free medium for 48 h and fixed 72 h after siRNA transfection. Bars, 5 μm (A–C). (B) GM130 and IFT20 localization in mIMCD3 cells expressing IFT20-GFP. Cells were cultured in serum-free DMEM and treated with dimethyl sulfoxide (DMSO; Ctl.) or PF670462 (1 μM) for 3 h. (C) Polycystin-2, IFT20, and γ-tubulin localization in mIMCD3 cells expressing IFT20-GFP. Cells were cultured in serum-free DMEM and treated with DMSO (Ctl.) or PF670462 (1 μM) for 3 h. (D) Quantitative analysis of polycystin-2 and γ-tubulin colocalization as indicated by Pearson's *r*. *t* test, $*p < 0.05$; $N = 12$ and 17 in DMSO and PF670462 treatment groups, respectively.

documented a sharp contrast between the effects of CK1δ and CK1ε knockdown, clearly indicating that CK1ε did not facilitate ciliogenesis in our model systems. This dichotomy of function was consistent with observations previously made regarding the specific role of CK1δ in Wnt3a-dependent neurite outgrowth (Greer and Rubin, 2011).

Numerous studies implicate CK1δ in various forms of polarized transport. The CK1δ orthologue in yeast, Hrr25p, supports the directionality of endoplasmic reticulum–Golgi traffic by phosphorylating the Sec23p/Sec24p coat complex (Lord *et al.*, 2011). Snapin, another CK1δ substrate, is a soluble *N*-ethylmaleimide–sensitive factor attachment protein receptor–associated protein that is believed to participate in exocytosis of cellular transport vesicles (Wolff *et al.*, 2006). CK1δ was reported to mediate repositioning of the centrosome in T-cells during formation of the immune synapse (Zyss *et al.*, 2011), a process that resembles ciliogenesis (Finetti *et al.*, 2009) and requires Rab11 (Gorska *et al.*, 2009). The mechanism involved CK1δ phosphorylation of end-binding protein 1, a plus end MT–associated protein that also participates in ciliogenesis (Schroder *et al.*, 2007, 2011). Of interest, another CK1δ substrate, Dishevelled (McKay *et al.*, 2001), is essential for apical positioning of the basal body in multiciliated *Xenopus* embryo epidermal cells (Park *et al.*, 2008), although there is no evidence that phosphorylation by CK1δ is involved. Future study of CK1δ activity is likely to provide insights into ciliogenesis and other processes that rely on polarized trafficking such as cell migration and cell division.

MATERIALS AND METHODS

Cell culture

hTERT-RPE cells, hTERT-RPE cells stably expressing GFP-Rab8a (Westlake *et al.*, 2011) or GFP-Rab11a, mIMCD3 cells, mIMCD3 cells stably expressing IFT20-GFP (Follit *et al.*, 2006), and MEF cells were maintained in DMEM supplemented with 10% fetal bovine serum (FBS), 100 U/ml penicillin, and 100 μg/ml streptomycin in a 5% CO_2, humidified, 37°C cell culture incubator. GFP-Rab11a was stably expressed in RPE FRT cell lines using the GLAP1 FRT vector as previously described (Sang *et al.*, 2011). Similarly, IFT20-GFP was stably expressed in RPE FRT cell lines using the GLAP7 FRT vector.

Isolation of MEF cells from mouse embryo

Mice carrying a *Csnk1d* floxed allele (B6.129S4-*Csnk1dtm1Drw*/J, stock number

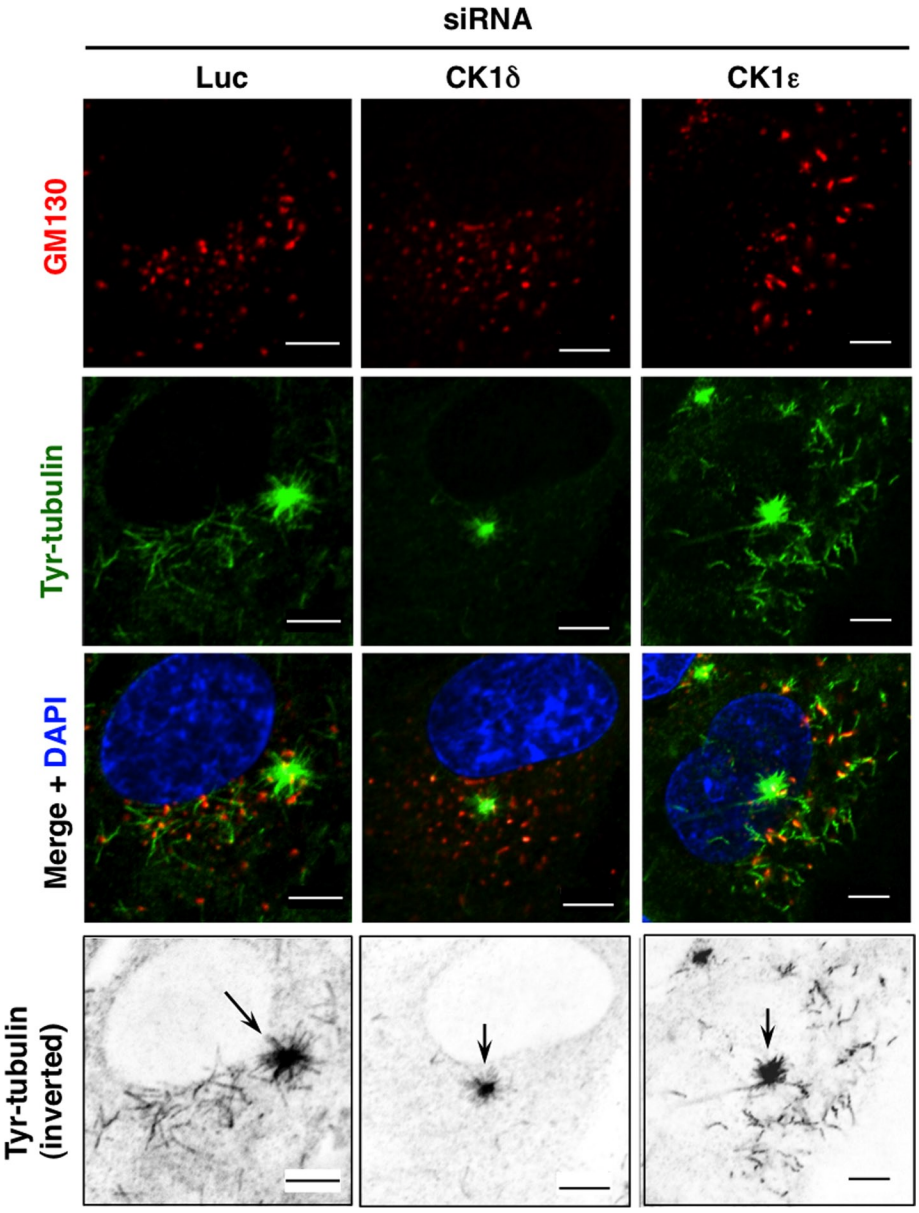

FIGURE 7: CK1δ siRNA inhibited MT nucleation at the Golgi. hTERT-RPE cells were transfected with the indicated siRNA reagents and 48 h later were treated with nocodazole (10 μM) for 2 h at 37°C. Nocodazole-containing medium was removed and cells were washed three times with cold DMEM and then incubated in warmed DMEM at 37°C for 3 min. Cells were fixed in cold methanol and stained for GM130, γ-tubulin, tyrosinated tubulin (indicator of newly formed MTs), and DNA. Bottom, micrographs showing tyrosinated tubulin signal in gray scale. Arrows indicate location of centrosome. Bars, 5 μm.

010487; Etchegaray *et al.*, 2009) were obtained from the Jackson Laboratory (Bar Harbor, ME). Embryonic day 12.5 (E12.5) embryos homozygous for the floxed allele were harvested, and heads and all internal organs were removed. The remaining tissues (trunk and limbs) were digested with 0.25% trypsin for 30 min and subsequently homogenized by trituration. Digested tissues were transferred into a flask containing warm DMEM supplemented with 10% FBS, and medium was replaced the next day. Once confluent, the primary MEF cells were collected and stored at –80°C for short-term use or in a liquid nitrogen tank for long-term applications. To generate *Csnk1d*-null or control MEFs, cells were infected with adenovirus encoding Cre recombinase (Ad-Cre) or GFP (Ad-GFP), respectively (Viral Technology Group, SAIC-Frederick, Frederic, MD). Once MEF cells were infected with adenovirus, they were used for ≤10 passages.

Isolation of RPE layer and retinal tissue from mouse embryos for immunostaining

Eyes were removed from killed E18.5 embryos and incubated for 20 min in 1× phosphate-buffered saline (PBS) at 4°C to facilitate dissection of the RPE layer from the remaining retinal tissue using a Zeiss Stereoscope (Stemi 2000-c; Zeiss, Jena, Germany). Both specimens were fixed in 4% paraformaldehyde for 30 min at room temperature. After washing with 1× PBS, RPE and retinal tissues were immunostained with the indicated reagents using the standard protocol (see later description), and flat mounts of stained tissues were imaged by confocal microscopy.

Ciliogenesis assays

To induce primary ciliogenesis, hTERT-RPE cells that had been grown on coverslips to 90% confluency were serum starved for 48 h and processed for immunostaining. For siRNA experiments, growth medium was replaced with serum-free DMEM 24 h after transfection, and cells were maintained for 48 h in this medium before processing for confocal microscopy. To examine the effect of PF670462 on ciliogenesis, hTERT-RPE and mIMCD3 cells were cultured in serum-free DMEM containing different concentrations of the kinase inhibitor for 48 h. MEF cells were not subjected to serum starvation in ciliogenesis assays. When experiments involved the use of DNA constructs, cells were processed for Western blotting or immunostaining 48 h after transfection.

Chemicals

See Supplemental Table S1.

siRNA reagents and transfection

For CK1δ knockdown, four different siRNA reagents were used independently. For CK1ε knockdown, two different siRNA reagents were used independently. A luciferase siRNA was synthesized by Dharmacon (Lafayette, CO) and used as negative control. See Supplemental Table S1 for sequence information. siRNA transfection experiments in hTERT-RPE cells were performed with the Amaxa system (Amaxa, Cologne, Germany) according to the manufacturer's protocol, using 200 pmol of siRNA/10^6 cells, with Nucleofector V (VACA-0003), program X-001. The effects of siRNA treatment were analyzed 48–72 h after transfection.

Recombinant DNA and transfection

pcDNA3.3 6xMyc-mouse CK1δ WT and ΔCT (lacking C-terminal domain), δCT-EGFP, and εCT-EGFP were previously described (Greer

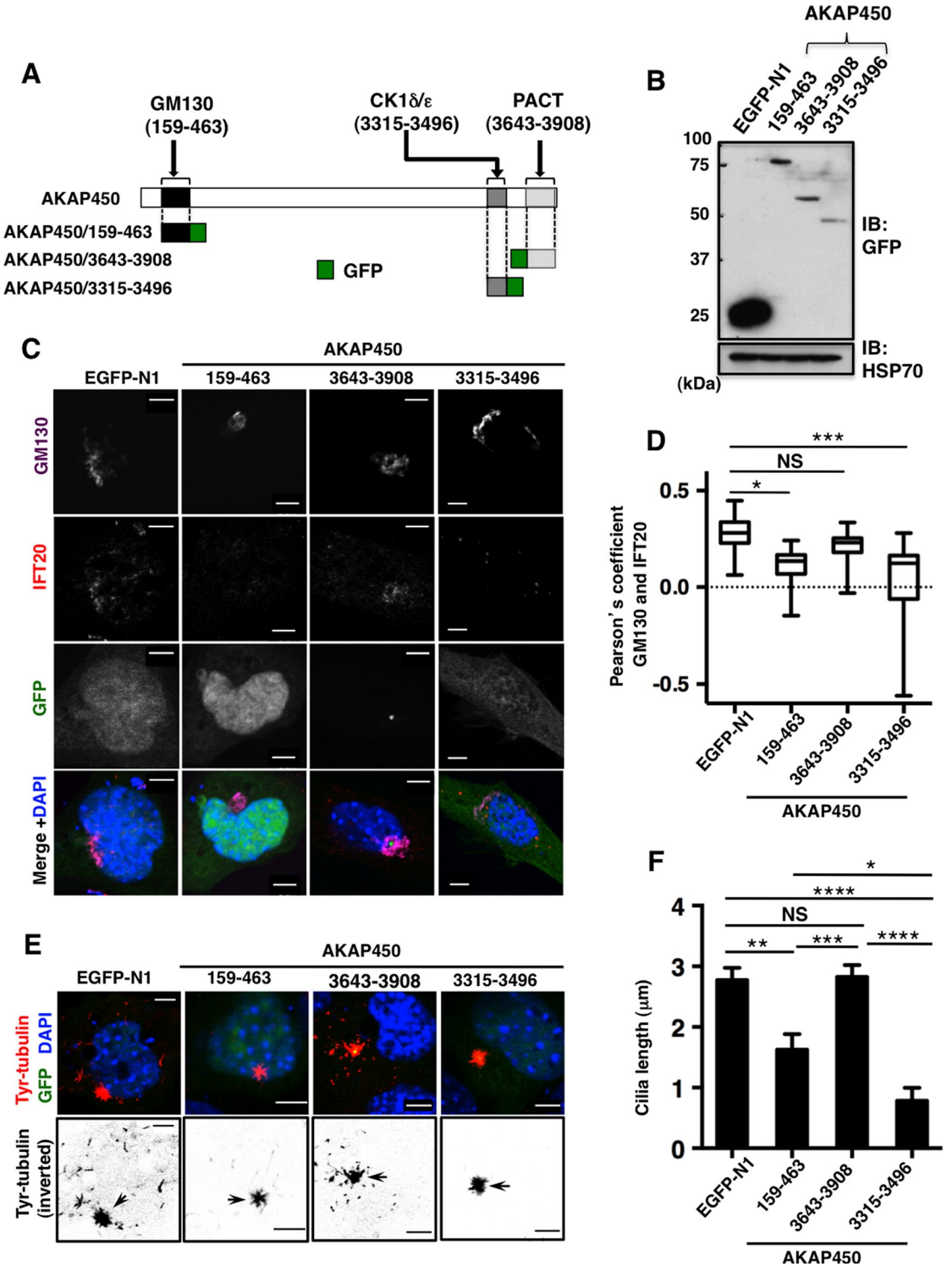

FIGURE 8: CK1δ-binding AKAP450 fragment inhibited IFT20 Golgi distribution, Golgi-derived MT nucleation and ciliogenesis. (A) Schematic diagram of GFP-labeled AKAP450 fragments. (B) Western blot analysis of AKAP450 fragments and EGFP expressed in MEF$^{Ctl.}$ cells. HSP70 was a loading control. (C) GM130 and IFT20 localization in MEF$^{Ctl.}$ cells expressing AKAP450 fragments or EGFP. Bars, 5 μm. (D) Quantitative analysis of GM130 and IFT20 colocalization illustrated in C. $N = 11$, 18, 15, and 15 for treatment groups from left to right. One-way ANOVA, $p < 0.001$; Tukey's test, $^*p < 0.05$, $^{***}p < 0.001$, NS = not significant. (E) Golgi-derived MT nucleation in MEF$^{Ctl.}$ cells transfected with GFP-labeled AKAP450 fragments. At 48 h after DNA transfection, MEF$^{Ctl.}$ cells were incubated with nocodazole (10 μM) for 2 h and then washed and processed as described in the legend to Figure 7. Representative micrographs show cells fixed after 5 min of recovery. Bars, 5 μm. (F) Ciliary length in MEF$^{Ctl.}$ cells transfected with GFP-labeled AKAP450 fragments. At 48 h after DNA transfection, cells were fixed and processed as described in *Materials and Methods*. $N = 49$, 50, 52, and 52 cells for treatment groups from left to right. One-way ANOVA, $p < 0.0001$; Tukey's test, $^*p < 0.05$, $^{**}p < 0.01$, $^{***}p < 0.001$, $^{****}p < 0.0001$, NS = not significant. See also Supplemental Figure S7.

and Rubin, 2011). CK1δ K38A, a kinase-inactive form, was generated by site-directed mutagenesis according to manufacturer's protocol (Quik-Change II; Agilent Technologies, Santa Clara, CA). IFT20-GFP was PCR amplified from pEGFP-N1-IFT20 (JAF 2.13; Follit *et al.*, 2006), cloned into pENTR/D-TOPO vector, and subsequently recloned into GLAP7 vector using LR clonase reaction in the Gateway cloning system (Invitrogen, Carlsbad, CA). AKAP450/159-463-GFP (numbering based on National Center for Biotechnology Information [NCBI] reference sequence NP_671714.1) and GFP-AKAP450/3643-3908 (numbering based on GenBank, CAB40713.1) constructs were kind gifts from Irina Kaverina (Vanderbilt University, Nashville, TN) and Sean Munro (MRC Laboratory of Molecular Biology, Cambridge, United Kingdom), respectively. To generate AKAP450/3315-3496-GFP (numbering based on NCBI reference sequence NP_671714.1), the corresponding AKAP450 fragment was amplified from hTERT-RPE cDNA by PCR. Primers contained *Hin*dIII and *Bam*HI sites at the 5′ and 3′ ends, respectively; PCR product was digested with these enzymes and ligated into pEGFP-N1 that was similarly digested. Sequences of new constructs were verified by analysis in the DNA Sequencing MiniCore Facility at the National Cancer Institute. (Bethesda, MD). For DNA transfection in MEF cells, Lipofectamine LTX with Plus reagent (15338030; Invitrogen) was used according to manufacturer's protocol.

Antibodies used for Western blotting and immunostaining

See Supplemental Table S1.

Immunoblotting

Eighty to 90% confluent monolayers that had been seeded in 6- or 12-well cell culture plates were rinsed twice with PBS, lysed, and processed for SDS–PAGE and Western blot analysis as previously described (Greer and Rubin, 2011). For immunoblot analysis to verify siRNA knockdown of endogenous proteins, hTERT-RPE cells that had been transfected with siRNA reagents were seeded in 6- or 12-well cell culture plates and harvested 48–72 h after transfection.

Immunofluorescence analysis

To visualize cilia, cells cultured on 12-mm-diameter glass coverslips (Fisher, Pittsburgh, PA) were first washed once with PBS and then with PHEM (60 mM Na–1,4-piperazinediethanesulfonic acid, 25 mM Na–4-(2-hydroxyethyl)-1-piperazineethanesulfonic acid, 10 mM Na–ethylene glycol tetraacetic acid, and 2 mM $MgCl_2$, pH 6.9), followed by treatment with PHEM containing 0.19 M NaCl, 1% saponin, 10 μM Taxol, and 0.1% dimethyl sulfoxide for 5 min at room temperature to permeabilize cells and stabilize tubulin. Cultures were then immersed in cold 100% MeOH at −30°C for 10 min, rehydrated by rinsing three times with PBS, and treated with blocking solution for 30 min at 37°C. As blocking solution, 6% BSA in PBS (for secondary antibody/antibodies produced in goat) or donkey serum (for secondary antibody/antibodies produced in donkey) was used. Primary antibody/antibodies was/were added with blocking solution, and samples were incubated for 1 h at 37°C or overnight at 4°C. After washing three times with PBS, samples were incubated with secondary antibody reagent(s) and 4′,6-diamidino-2-phenylindole (DAPI) with blocking solution for 45 min at room temperature. After three washes PBS, coverslips were mounted on glass slides (VWR Scientific, Radnor, PA) using ProLong Gold Antifade reagent (P36930; Invitrogen). To perform immunostaining in GFP-expressing cells, formaldehyde/paraformaldehyde fixation was used instead of MeOH to preserve GFP signal (Figures 2, F–H, 3, 6, A–C, and 8F and Supplemental Figures S3, S5, and S7). After washing with PBS and PHEM, cells were fixed with freshly prepared 3.7% formaldehyde and 1% Triton X-100 in PHEM supplemented with Taxol (10 μM) for 10 min at room temperature. Cells were washed and blocked, followed by the same procedure as described after MeOH fixation. For experiments presented in Figures 4, A–C, and 5, A–E and H–I, and Supplemental Figures S1A and S4, cells were fixed with cold 100% MeOH, followed by blocking and antibody treatment. For Supplemental Figure S1B, cells were fixed with 3.7% formaldehyde at room temperature for 15 min and treated with 0.1% Triton X-100 for 10 min, followed by blocking and antibody treatment. In experiments presented in Figure 8C, cells were fixed with 4% paraformaldehyde at room temperature for 15 min and treated with 0.1% Triton X-100 for 10 min, followed by blocking and antibody treatment.

MT regrowth assays

Cells grown on coverslips were treated with nocodazole (10 μM) in serum-containing DMEM at 37°C for 2 h; then nocodazole was washed out three times with cold, serum-free DMEM. After warm (room temperature) medium was added, cells were returned to 37°C/CO_2 incubator and harvested at different times (1, 3, 5, 7 min) by applying either cold 100% MeOH (for Figure 7 and Supplemental Figure S6) or cold PHEM (containing 3.7% formaldehyde, 1% Triton X-100, and 10 μM Taxol for Figure 8E) and maintenance at −20°C for 10 min or on ice for 10 min, respectively. Cells were washed with PBS, blocked, and incubated with primary antibodies (tyrosinated tubulin, γ-tubulin, GM130), followed by incubation with secondary antibodies (and DAPI when needed).

Cell imaging, measurement of ciliary length, and analysis of Golgi morphology

Fluorescence images were collected with a laser-scanning confocal microscope (510 LSCM) and a 63× objective (Carl Zeiss, Jena, Germany). Zeiss LSM image browser, version 4.0.0.157, was used for image processing, and composite figures were prepared with PhotoShop CS3, version 10.0.1 (Adobe Systems, San Jose, CA). Images of cilia were viewed with ImageJ, version 1.47k (http://imagej.nih.gov/ij), and ciliary length was measured using its line tool. Depending on the form of cilia, straight, segmented, or freehand line was chosen. Golgi apparatus diameter and centrosome–Golgi distance were measured as previously reported (Hurtado *et al.*, 2011), using ImageJ software. Colocalization was examined using Colocalization Finder in ImageJ (http://rsbweb.nih.gov/ij/plugins/colocalization-finder.html).

Statistical analysis

The significance of differences in data was determined with Student's *t* test or one-way analysis of variance (ANOVA) followed by Tukey's test or Fisher's exact test, depending on experiments (see figure legends). The differences were considered to be significant for $p < 0.05$.

ACKNOWLEDGMENTS

We thank Eli Lilly for providing the CK1δ monoclonal antibody 128A and Irina Kaverina and Sean Munro, respectively, for providing the plasmids encoding AKAP450/159-463-GFP and GFP-AKAP450/3643-3908. We also appreciate comments on the manuscript from Sergei Sokol and Kyeongmi Kim (Mount Sinai School of Medicine, New York, NY). This research was supported by Grant GM060992 from the National Institutes of Health to G.J.P. and the Intramural Research Program of the National Institutes of Health, National Cancer Institute.

REFERENCES

Behrend L, Stoter M, Kurth M, Rutter G, Heukeshoven J, Deppert W, Knippschild U (2000). Interaction of casein kinase 1 delta (CK1delta) with post-Golgi structures, microtubules and the spindle apparatus. Eur J Cell Biol 79, 240–251.

Berbari NF, Lewis JS, Bishop GA, Askwith CC, Mykytyn K (2008). Bardet-Biedl syndrome proteins are required for the localization of G protein-coupled receptors to primary cilia. Proc Natl Acad Sci USA 105, 4242–4246.

Bischof J, Muller A, Fander M, Knippschild U, Fischer D (2011). Neurite outgrowth of mature retinal ganglion cells and PC12 cells requires activity of CK1delta and CK1epsilon. PLoS One 6, e20857.

Cheong JK, Virshup DM (2011). Casein kinase 1: complexity in the family. Int J Biochem Cell Biol 43, 465–469.

Coppieters F, Lefever S, Leroy BP, De Baere E (2010). CEP290, a gene with many faces: mutation overview and presentation of CEP290base. Hum Mutat 31, 1097–1108.

Dammermann A, Merdes A (2002). Assembly of centrosomal proteins and microtubule organization depends on PCM-1. J Cell Biol 159, 255–266.

DeMaggio AJ, Lindberg RA, Hunter T, Hoekstra MF (1992). The budding yeast HRR25 gene product is a casein kinase I isoform. Proc Natl Acad Sci USA 89, 7008–7012.

Efimov A *et al*. (2007). Asymmetric CLASP-dependent nucleation of noncentrosomal microtubules at the *trans*-Golgi network. Dev Cell 12, 917–930.

Etchegaray JP *et al*. (2009). Casein kinase 1 delta regulates the pace of the mammalian circadian clock. Mol Cell Biol 29, 3853–3866.

Finetti F, Paccani SR, Riparbelli MG, Giacomello E, Perinetti G, Pazour GJ, Rosenbaum JL, Baldari CT (2009). Intraflagellar transport is required for polarized recycling of the TCR/CD3 complex to the immune synapse. Nat Cell Biol 11, 1332–1339.

Fish KJ, Cegielska A, Getman ME, Landes GM, Virshup DM (1995). Isolation and characterization of human casein kinase I epsilon (CKI), a novel member of the CKI gene family. J Biol Chem 270, 14875–14883.

Follit JA, Tuft RA, Fogarty KE, Pazour GJ (2006). The intraflagellar transport protein IFT20 is associated with the Golgi complex and is required for cilia assembly. Mol Biol Cell 17, 3781–3792.

Garcia-Gonzalo FR *et al*. (2011). A transition zone complex regulates mammalian ciliogenesis and ciliary membrane composition. Nat Genet 43, 776–784.

Garcia-Gonzalo FR, Reiter JF (2012). Scoring a backstage pass: mechanisms of ciliogenesis and ciliary access. J Cell Biol 197, 697–709.

Gault WJ, Olguin P, Weber U, Mlodzik M (2012). *Drosophila* CK1-gamma, gilgamesh, controls PCP-mediated morphogenesis through regulation of vesicle trafficking. J Cell Biol 196, 605–621.

Gerdes JM, Davis EE, Katsanis N (2009). The vertebrate primary cilium in development, homeostasis, and disease. Cell 137, 32–45.

Gillingham AK, Munro S (2000). The PACT domain, a conserved centrosomal targeting motif in the coiled-coil proteins AKAP450 and pericentrin. EMBO Rep 1, 524–529.

Gorska MM, Liang Q, Karim Z, Alam R (2009). Uncoordinated 119 protein controls trafficking of Lck via the Rab11 endosome and is critical for immunological synapse formation. J Immunol 183, 1675–1684.

Greer YE, Rubin JS (2011). Casein kinase 1 delta functions at the centrosome to mediate Wnt-3a-dependent neurite outgrowth. J Cell Biol 192, 993–1004.

Gross SD, Anderson RA (1998). Casein kinase I: spatial organization and positioning of a multifunctional protein kinase family. Cell Signal 10, 699–711.

Hsiao YC, Tuz K, Ferland RJ (2012). Trafficking in and to the primary cilium. Cilia 1, 4.

Hurtado L, Caballero C, Gavilan MP, Cardenas J, Bornens M, Rios RM (2011). Disconnecting the Golgi ribbon from the centrosome prevents directional cell migration and ciliogenesis. J Cell Biol 193, 917–933.

Ikeda K, Zhapparova O, Brodsky I, Semenova I, Tirnauer JS, Zaliapin I, Rodionov V (2011). CK1 activates minus-end-directed transport of membrane organelles along microtubules. Mol Biol Cell 22, 1321–1329.

Jakobsen L *et al*. (2011). Novel asymmetrically localizing components of human centrosomes identified by complementary proteomics methods. EMBO J 30, 1520–1535.

Kim S, Dynlacht BD (2013). Assembling a primary cilium. Curr Opin Cell Biol 25, 506–511.

Kim J, Krishnaswami SR, Gleeson JG (2008). CEP290 interacts with the centriolar satellite component PCM-1 and is required for Rab8 localization to the primary cilium. Hum Mol Genet 17, 3796–3805.

Knippschild U, Gocht A, Wolff S, Huber N, Lohler J, Stoter M (2005). The casein kinase 1 family: participation in multiple cellular processes in eukaryotes. Cell Signal 17, 675–689.

Knodler A, Feng S, Zhang J, Zhang X, Das A, Peranen J, Guo W (2010). Coordination of Rab8 and Rab11 in primary ciliogenesis. Proc Natl Acad Sci USA 107, 6346–6351.

Lopes CA, Prosser SL, Romio L, Hirst RA, O'Callaghan C, Woolf AS, Fry AM (2011). Centriolar satellites are assembly points for proteins implicated in human ciliopathies, including oral-facial-digital syndrome 1. J Cell Sci 124, 600–612.

Lord C, Bhandari D, Menon S, Ghassemian M, Nycz D, Hay J, Ghosh P, Ferro-Novick S (2011). Sequential interactions with Sec23 control the direction of vesicle traffic. Nature 473, 181–186.

Marshall WF (2008). The cell biological basis of ciliary disease. J Cell Biol 180, 17–21.

McKay RM, Peters JM, Graff JM (2001). The casein kinase I family in Wnt signaling. Dev Biol 235, 388–396.

Murakami A, Kimura K, Nakano A (1999). The inactive form of a yeast casein kinase I suppresses the secretory defect of the sec12 mutant. Implication of negative regulation by the Hrr25 kinase in the vesicle budding from the endoplasmic reticulum. J Biol Chem 274, 3804–3810.

Nachury MV, Seeley ES, Jin H (2010). Trafficking to the ciliary membrane: how to get across the periciliary diffusion barrier? Annu Rev Cell Dev Biol 26, 59–87.

Park TJ, Mitchell BJ, Abitua PB, Kintner C, Wallingford JB (2008). Dishevelled controls apical docking and planar polarization of basal bodies in ciliated epithelial cells. Nat Genet 40, 871–879.

Pedersen LB, Rosenbaum JL (2008). Intraflagellar transport (IFT) role in ciliary assembly, resorption and signalling. Curr Top Dev Biol 85, 23–61.

Rivero S, Cardenas J, Bornens M, Rios RM (2009). Microtubule nucleation at the cis-side of the Golgi apparatus requires AKAP450 and GM130. EMBO J 28, 1016–1028.

Sang L *et al*. (2011). Mapping the NPHP-JBTS-MKS protein network reveals ciliopathy disease genes and pathways. Cell 145, 513–528.

Satir P, Christensen ST (2007). Overview of structure and function of mammalian cilia. Annu Rev Physiol 69, 377–400.

Schroder JM *et al*. (2011). EB1 and EB3 promote cilia biogenesis by several centrosome-related mechanisms. J Cell Sci 124, 2539–2551.

Schroder JM, Schneider L, Christensen ST, Pedersen LB (2007). EB1 is required for primary cilia assembly in fibroblasts. Curr Biol 17, 1134–1139.

Sillibourne JE, Milne DM, Takahashi M, Ono Y, Meek DW (2002). Centrosomal anchoring of the protein kinase CK1delta mediated by attachment to the large, coiled-coil scaffolding protein CG-NAP/AKAP450. J Mol Biol 322, 785–797.

Stowe TR, Wilkinson CJ, Iqbal A, Stearns T (2012). The centriolar satellite proteins Cep72 and Cep290 interact and are required for recruitment of BBS proteins to the cilium. Mol Biol Cell 23, 3322–3335.

Thyberg J, Moskalewski S (1999). Role of microtubules in the organization of the Golgi complex. Exp Cell Res 246, 263–279.

Westlake CJ *et al*. (2011). Primary cilia membrane assembly is initiated by Rab11 and transport protein particle II (TRAPPII) complex-dependent trafficking of Rabin8 to the centrosome. Proc Natl Acad Sci USA 108, 2759–2764.

Westlake CJ, Junutula JR, Simon GC, Pilli M, Prekeris R, Scheller RH, Jackson PK, Eldridge AG (2007). Identification of Rab11 as a small GTPase binding protein for the Evi5 oncogene. Proc Natl Acad Sci USA 104, 1236–1241.

Wolff S, Stoter M, Giamas G, Piesche M, Henne-Bruns D, Banting G, Knippschild U (2006). Casein kinase 1 delta (CK1delta) interacts with the SNARE associated protein snapin. FEBS Lett 580, 6477–6484.

Yadav S, Puri S, Linstedt AD (2009). A primary role for Golgi positioning in directed secretion, cell polarity, and wound healing. Mol Biol Cell 20, 1728–1736.

Zyss D, Ebrahimi H, Gergely F (2011). Casein kinase I delta controls centrosome positioning during T cell activation. J Cell Biol 195, 781–797.